

# Synthesis and characterization of collagen/hydroxyapatite:magnetite composite material for bone cancer treatment

Ecaterina Andronescu · Maria Fikai ·  
Georgeta Voicu · Denisa Fikai ·  
Maria Maganu · Anton Fikai

Received: 28 October 2009 / Accepted: 29 March 2010 / Published online: 7 April 2010  
© Springer Science+Business Media, LLC 2010

**Abstract** Our purpose was obtaining and characterizing a complex composite system with multifunctional role: bone graft material and hyperthermia generator necessary for bone cancer therapy. The designed system was a magnetite enriched collagen/hydroxyapatite composite material, obtained by a co-precipitation method. Due to the applied electromagnetic field the magnetite will induce hyperthermia and cause tumoral cell apoptosis. The complex bone graft system was characterised by XRD, FTIR and SEM, while the hyperthermia was quantify by measuring the temperature increase due to the applied alternative electromagnetic field.

## 1 Introduction

Magnetite is one of the most studied magnetic materials due to their biomedical application (Fig. 1): magnetic resonance imaging (MRI) as magnetic contrast agent [1]; drug delivery and drug carrier [2, 3] and hyperthermia [4].

Many times, bone cancer treatment involves two stages. In the first stage the tumoral bone tissue is surgically removed [5]. After the surgical intervention, the obtained bone defect can be filled with bone graft material or better with magnetite or anti-tumoral loaded bone graft material.

The most cases of tumours recurrence are done due to the partial removal of tumoral tissue. This is the reason because all the time the surgical interventions are accomplished by chemo/radiotherapy. The bone cancer treatment can be represented as summarised in Fig. 2.

In present, a lot of composite materials with different content of magnetite were obtained [6–9] in order to induce hyperthermia. Also, many anti-tumoral drug delivery systems were obtained [10–20] some of them containing gold/silver nanoparticles with proved antitumoral activity [21–23].

## 2 Experimental

Collagen (300,000 Da) gel was obtained in the Leather and Footwear Research Institute, Collagen Department starting from calf hides by chemical and enzymatic extraction. The collagen gel concentration was 1.6% and pH = 7.

Collagen mineralization occurs in two stages, in order to mimic the in vivo osteosynthesis [24]. In the first stage the calcium hydroxide (Fluka) suspension is added onto the collagen gel and let to interact for 24 h. In the second stage, the corresponding amount of sodium dihydrogen phosphate is added (Ca:P molar ratio was 1.67) in order to precipitate pure HA. The amount of collagen, calcium hydroxide and sodium dihydrogen phosphate is added in order to obtain a composite material with the COLL: HA ratio of 1:4. The final pH was adjusted to ~9 with NaOH 0.1 M.

In order to obtain COLL/HA-Fe<sub>3</sub>O<sub>4</sub> composite materials the wet COLL/HA composite, obtained as presented above, is mixed with the appropriate amount of magnetite particle. The magnetite particles were obtained by co-precipitation from aqueous solution starting from FeCl<sub>3</sub> and

---

E. Andronescu · M. Fikai · G. Voicu · D. Fikai · A. Fikai (✉)  
Faculty of Applied Chemistry and Material Science, Politehnica  
University of Bucharest, 1-7 Polizu Street, 011061 Bucharest,  
Romania  
e-mail: anton\_fikai81@yahoo.com

M. Maganu  
Center of Organic Chemistry “Costin D. Nenitescu”, Romanian  
Academy, 202B Splaiul Independentei, 050461 Bucharest,  
Romania

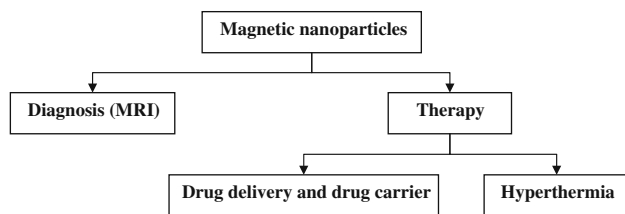


**Fig. 1** Applications of magnetic nanoparticle

$\text{FeSO}_4$  ( $\text{Fe}^{2+}:\text{Fe}^{3+}$  molar ratio was 1:2), as precursors (both purchased from Fluka) at pH  $\sim 9$ .

During the synthesis of COLL/HA–magnetite composite, the temperature was thermostated at  $35 \pm 2^\circ\text{C}$ . The composite materials were dried by freeze-drying.

Hyperthermia was obtained by due to the interaction of the composite materials with the electromagnetic field. The magnetic field was created using a horizontal coil, the applied frequency being 150 kHz.

The obtained material was investigated by X-ray diffraction, IR spectroscopy and scanning and transmission electron microscopy.

X-ray diffraction analysis was performed using a Shimadzu XRD 6000 diffractometer at room temperature. In all the cases, Cu  $K\alpha$  radiation from a Cu X-ray tube was used. The samples were scanned in the Bragg angle,  $2\theta$  range of 10–80.

For IR spectroscopy (Shimadzu 8400 FTIR Spectrometer) measurements, the spectra were recorded in the wave number range of  $400\text{--}4,000\text{ cm}^{-1}$ , with a resolution of  $2\text{ cm}^{-1}$ .

SEM analyses were performed on a HITACHI S2600N electron microscope on samples covered with silver layer.

The transmission electron images were obtained on finely powdered samples using a Tecnai<sup>TM</sup> G<sup>2</sup> F30 S-TWIN high resolution transmission electron microscope (HRTEM). The microscope was operated in transmission mode at 300 kV while TEM point resolution was 2 Å and line resolution was 1 Å.

### 3 Results and discussion

The composite material composition was confirmed by XRD, FTIR, EDS and DTA-TG.

**Fig. 2** Bone cancer treatment of osteosarcoma

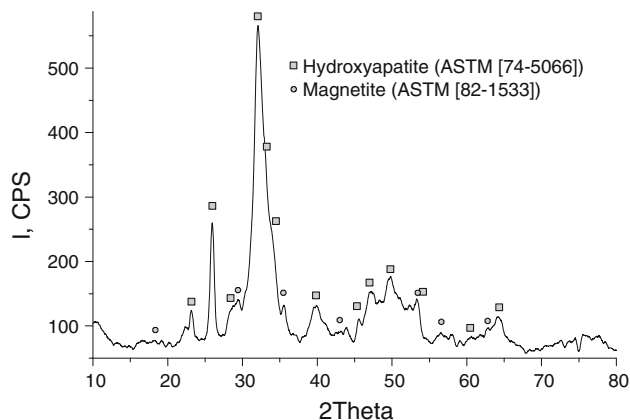
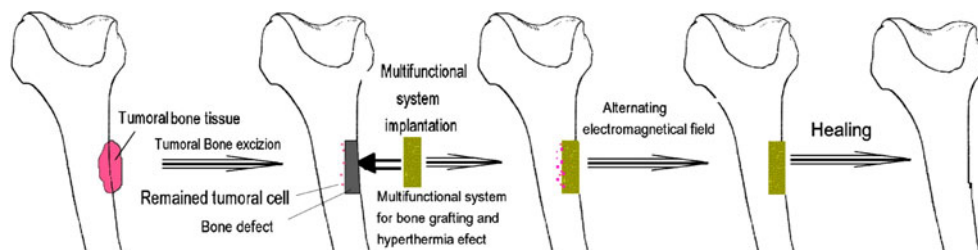


**Fig. 3** XRD pattern of COLL/HA– $\text{Fe}_3\text{O}_4$  composite material containing 2% magnetite

X-Ray diffraction was used in order to confirm the presence of HA and magnetite as pure phases (Fig. 3). It can be easily identify the main characteristic peaks of HA ( $2\theta = 25.90, 28.96, 31.79, 32.21, 32.92, 34.09, 39.82, 46.73$  and  $49.53$ ) and magnetite ( $2\theta = 30.04, 35.43, 43.05, 56.94$  and  $62.52$ ).

SEM images were recorded at different magnification on the materials surface and transversal section. At low magnification, the SEM images of COLL/HA– $\text{Fe}_3\text{O}_4$  composite (Fig. 4a, b) exhibit a homogenous structure, the images being very similar with the images recorded for COLLHA composite materials.

At relative high magnification, due to the special interactions between collagen and magnetite, acicular (rod-like) crystals can be observed (Fig. 4c, d). The size of the acicular crystals is in the range of a few  $\mu\text{m}$  in length and 100–300 nm in diameter.

The acicular structures formation can be explained based on the above presented synthesis procedure. After the addition of the calcium hydroxide suspension, the pH became basic and the collagen fibrillogenesis began [25]. When the magnetite particle is added, the collagen molecule is associated in fibrils and fibres and these will function as surfactants for magnetite stabilization. In same conditions of synthesis, in the absence of magnetite, the obtained COLL/HA composite materials exhibit no such acicular structures as we previously reported [26, 27].

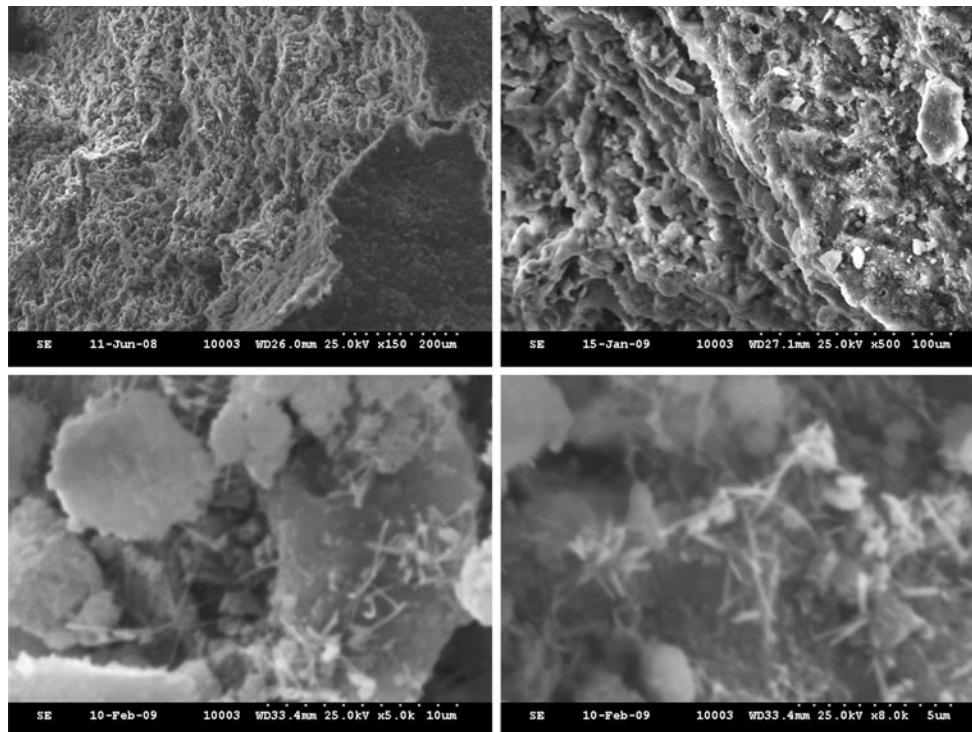


**Fig. 4** SEM images of COLL/HA-Fe<sub>3</sub>O<sub>4</sub> composite material

Comparing with the case of magnetite stabilization with citrate anions it can be observed a morphological change of the composite. If, in the case of citrate the stabilised magnetite particles are spherical, the stabilization in the presence of collagen (in the above presented conditions) leads to acicular morphology because the collagen fibrils and fibres are bigger than magnetite core and only a few collagen suprastructures can be bound (through electrostatic interactions) around the magnetite particle.

Also, SEM images give information about the porosity of the composite materials.

The above-mentioned theory is confirmed also by EDS analysis (Fig. 5). For this purpose we recorded the EDS spectra, at the same magnification, in acicular rich and, respectively, acicular free zone. Obviously quantitative

determination cannot be made with accuracy due to the low content of Fe<sub>3</sub>O<sub>4</sub>, the recorded spectra are suggestive. In any acicular rich zone, the Fe peak is present at about 6.3 keV while in the acicular free zone the Fe peak is absent.

Transmission electron microscopy is used in order to analyze the magnetite particles shape and size (Fig. 6). There can be identified two kinds of magnetite nanoparticles: spherical and rod-like. The dimension of the particles varies from ~5 nm and up to 20 nm, the mean diameter of these particles being ~10–12 nm while the rod-like nanoparticles can reach up to 50 nm length.

The infrared spectrum, recorded for COLL/HA-Fe<sub>3</sub>O<sub>4</sub> composite material (Fig. 7) confirms the characteristic peaks of the components, some of them being superposed.

**Fig. 5** EDS spectra of COLL/HA-Fe<sub>3</sub>O<sub>4</sub> composite material **a** acicular rich zone and **b** acicular free zone

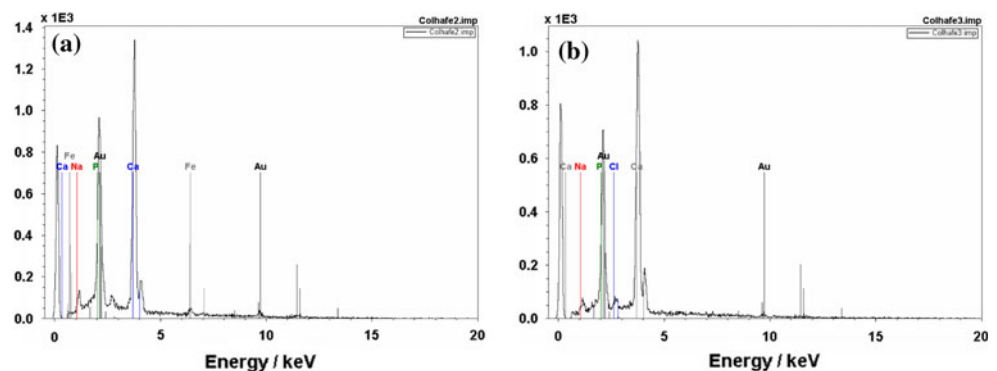


**Fig. 6** **a** TEM and **b** HRTEM image of magnetite nanoparticle

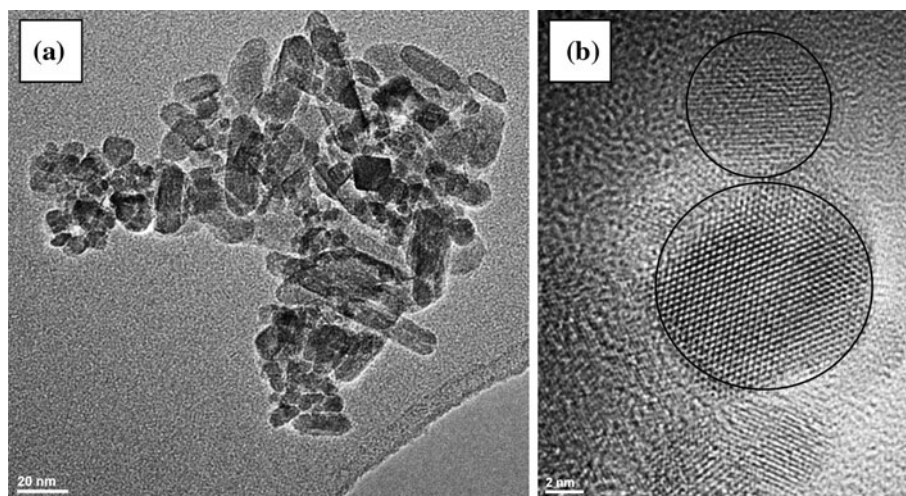
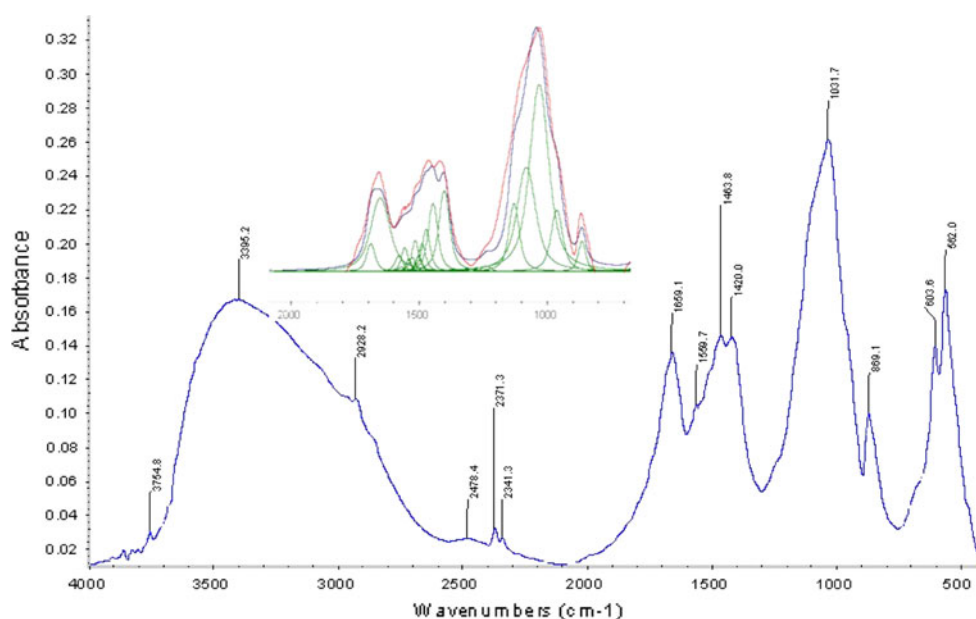


**Fig. 7** Infrared spectra of **a** COLL/HA-Fe<sub>3</sub>O<sub>4</sub> composite material; **b** deconvoluted spectrum of COLL/HA-Fe<sub>3</sub>O<sub>4</sub> composite material (range 700–2,000 cm<sup>-1</sup>)



In order to resolve these superposed peaks the composite spectrum was deconvoluted. After the spectrum deconvolution over the region of 400–1,800 cm<sup>-1</sup>, it can be clearly identify the collagen/hydroxyapatite main absorption bands [24] but also the main characteristic absorption bands of magnetite (713, 878, 962, 1,082 and 1,450 cm<sup>-1</sup>).

The obtained composite materials were analysed also from the point of view of the produced hyperthermia. In all three cases before measurements the composite materials were kept at 37°C for 1 h. Then, the composite materials were introduced in the electromagnetic field (frequency 150 kHz) and the temperature was determined after 5, 10, 15, 20, 30 and 60 min. It can be observed that increasing amount of magnetite lead to an increase thermal effect (Fig. 8).

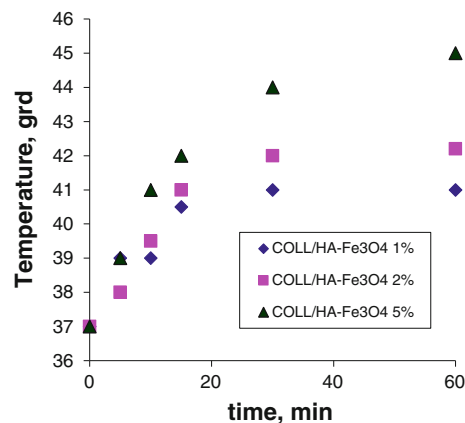


**Fig. 8** Temperature dependence of COLL/HA-Fe<sub>3</sub>O<sub>4</sub> with irradiation time (frequency = 150 kHz)



It is worth to mention that using the same magnetite nanoparticles (composition, shape and size distribution) the concentration can influence the obtained thermal effect. Even in small concentration of magnetic nanoparticle, the hyperthermia can be evidenced. In all the cases, the increase is adequate for the use of these composite materials for cancer treatment by hyperthermia. In case of bone cancer, these materials can be used for both regeneration and antitumoral effect.

#### 4 Conclusion

Our purpose was to obtain a regenerative composite material based on collagen and hydroxyapatite, which contain different concentration of magnetite nanoparticle. The role of magnetite is to produce controlled hyperthermia which can be activated by an alternative electromagnetic field, any time after implantation.

The rod-like structures characteristic only of the COLL/HA-Fe<sub>3</sub>O<sub>4</sub> composite material and not for COLL/HA can be explained based on the interactions occurred between collagen fibrils and fibres and magnetite.

It was obtained a multifunctional composite material in order to assure bone regeneration and antitumoral effect.

Obviously, the COLL/HA-Fe<sub>3</sub>O<sub>4</sub> composite materials containing 1 and 2% magnetite cannot produce the necessary hyperthermia; the COLL/HA-Fe<sub>3</sub>O<sub>4</sub> composite materials with higher content of magnetite (for instance 5%) can be successfully used as hyperthermia generator system, the activation time being of about 20–30 min (at 150 kHz).

In the future, we intend to reduce the necessary magnetite induced hyperthermia by the use of some more complex systems containing gold or silver nanoparticles with anti-tumoral activity. The combined effect of magnetite and gold/silver nanoparticles will improve the anti-tumoral effect and perhaps will permit to work with systems with lower content of magnetite without to reduce the global antitumoral effect.

**Acknowledgements** We are gratefully thanks to Chem. Madalina ALBU to provide us the collagen gel. This work was partially supported by Romanian National Authority for Scientific Research through project 72\_198/2008.

#### References

- Brahler M, Georgieva R, Buske N, Muller A, Muller S, Pinkernelle J, et al. Magnetite-loaded carrier erythrocytes as contrast agents for magnetic resonance imaging. *Nano Lett.* 2006; 6(11):2505–9.
- Lin CY, Ho KC. Synthesis of superparamagnetic magnetite nanoparticles for thermoresponsive drug delivery. *Nanotechnology.* 2007;2:405–8.
- Yang J, Lee H, Hyung W, Park S-B, Haam S. Magnetic PECA nanoparticles as drug carriers for targeted delivery: synthesis and release characteristics. *J Microencapsul.* 2006;23(2):203–12.
- Matsuoka F, Shinkai M, Honda H, Kubo T, Sugita T, Kobayashi T. Hyperthermia using magnetite cationic liposomes for hamster osteosarcoma. *Biomagn Res Technol.* 2004;2(1):3.
- Orentas R, Hodge JW, Johnson BD, editors. *Cancer vaccines and tumor immunity.* New York: Wiley; 2008.
- Li BQ, Jia DC, Zhou Y, Hu QL, Cai W. Magnetic hydroxyapatite/chitosan nanocomposites via in situ hybridization strategy. *Bioceramics.* 2007;330–332(Pts 1–2):357–60.
- Wu J, Hu QL, Chen FP, Li BQ, Shen JC. Study of the mechanical property of magnetite/hydroxyapatite/chitosan nano-composite. *Bioceramics.* 2007;330–332(Pts 1–2):435–8.
- Cui W, Hu QL, Wu J, Li BQ, Shen JC. Preparation and characterization of magnetite/hydroxyapatite/chitosan nanocomposite by in situ compositing method. *J Appl Polym Sci.* 2008;109(4): 2081–8.
- Murakami S, Hosono T, Jeyadevan B, Kamitakahara M, Ioku K. Hydrothermal synthesis of magnetite/hydroxyapatite composite material for hyperthermia therapy for bone cancer. *J Ceram Soc Jpn.* 2008;116(1357):950–4.
- Ruel-Gariepy E, Shive M, Bichara A, Berrada M, Le Garrec D, Chenite A, et al. A thermosensitive chitosan-based hydrogel for the local delivery of paclitaxel. *Eur J Pharm Biopharm.* 2004; 57(1):53–63.
- Yan XL, Gemeinhart RA. Cisplatin delivery from poly(acrylic acid-co-methyl methacrylate) microparticles. *J Control Release.* 2005;106(1–2):198–208.
- Ta HT, Dass CR, Dunstan DE. Injectable chitosan hydrogels for localised cancer therapy. *J Control Release.* 2008;126(3):205–16.
- Reddy LH, Sharma RK, Chuttani K, Mishra AK, Murthy RSR. Influence of administration route on tumor uptake and biodistribution of etoposide loaded solid lipid nanoparticles in Dalton's lymphoma tumor bearing mice. *J Control Release.* 2005;105(3): 185–98.
- Miyazaki T, Yomota C, Okada S. Development and release characterization of hyaluronan-doxycycline gels based on metal coordination. *J Control Release.* 2001;76(3):337–47.
- Konishi M, Tabata Y, Kariya M, Hosseinkhani H, Suzuki A, Fukuhara K, et al. In vivo anti-tumor effect of dual release of cisplatin and adriamycin from biodegradable gelatin hydrogel. *J Control Release.* 2005;103(1):7–19.
- Kim JH, Kim YS, Park K, Lee S, Nam HY, Min KH, et al. Antitumor efficacy of cisplatin-loaded glycol chitosan nanoparticles in tumor-bearing mice. *J Control Release.* 2008;127(1): 41–9.
- Harashima H, Iida S, Urakami Y, Tsuchihashi M, Kiwada H. Optimization of anti-tumor effect of liposomally encapsulated doxorubicin based on simulations by pharmacokinetic/pharmacodynamic modeling. *J Control Release.* 1999;61(1–2):93–106.
- Cafaggi S, Russo E, Stefani R, Leardi R, Caviglioli G, Parodi B, et al. Preparation and evaluation of nanoparticles made of chitosan or N-trimethyl chitosan and a cisplatin-alginate complex. *J Control Release.* 2007;121(1–2):110–23.
- Wang JP, Takayama K, Nagai T, Maitani Y. Pharmacokinetics and antitumor effects of vincristine carried by microemulsions composed of PEG-lipid, oleic acid, vitamin E and cholesterol. *Int J Pharm.* 2003;251(1–2):13–21.
- Netz DJA, Sepulveda P, Pandolfelli VC, Spadaro ACC, Alencastre JB, Bentley MVLB, et al. Potential use of gelcasting hydroxyapatite porous ceramic as an implantable drug delivery system. *Int J Pharm.* 2001;213(1–2):117–25.
- Xu R, Ma J, Sun XC, Chen ZP, Jiang XL, Guo ZR, et al. Ag nanoparticles sensitize IR-induced killing of cancer cells. *Cell Res.* 2009;19(8):1031–4.

22. Melnikov OV, Gorbenko OY, Markelova MN, Kaul AR, Atsarkin VA, Demidov VV, et al. Ag-doped manganite nanoparticles: new materials for temperature-controlled medical hyperthermia. *J Biomed Mater Res A*. 2009;91A(4):1048–55.
23. Paciotti GF, Myer L, Weinreich D, Goia D, Pavel N, McLaughlin RE, et al. Colloidal gold: a novel nanoparticle vector for tumor directed drug delivery. *Drug Deliv*. 2004;11(3):169–83.
24. Fikai A, Andronescu E, Ghitulica C, Voicu G, Trandafir V, Manzu D, et al. Collagen/hydroxyapatite interactions in composite biomaterials. *Mater Plast*. 2009;46(1):11–5.
25. Li Y, Asadi A, Monroe MR, Douglas EP. pH effects on collagen fibrillogenesis in vitro: electrostatic interactions and phosphate binding. *Mater Sci Eng C*. 2009;29(5):1643–9.
26. Fikai A, Andronescu E, Voicu G, Ghitulica C, Fikai D. The influence of collagen support and ionic species on the morphology of collagen/hydroxyapatite composite materials. *Mater Charact*. 2010;61:402–7. doi:[10.1016/j.matchar.2010.01.003](https://doi.org/10.1016/j.matchar.2010.01.003).
27. Fikai A, Andronescu E, Trandafir V, Ghitulica C, Voicu G. Collagen/hydroxyapatite composite obtained by electric field orientation. *Mater Lett*. 2010;64(4):541–4.